BMC Musculoskeletal Disorders

RESEARCH

Open Access

Teriparatide facilitates osteogenic differentiation of bone mesenchymal stem cells to alleviate idiopathic osteoporosis via the circFNDC3B-miR-125a-5p-GLS axis

Jiaxin Fu[1,2,3,4,5*], Zhi Liu[1,2,3,4], Guangxin Zhang[1,2,3,4] and Chun Zhang[1,2,3,4]

Abstract

Osteoporosis (OP), a systemic bone disease, is characterized by degeneration of bone microstructure and susceptibility to fracture. Teriparatide (TPD) is an active fragment of human endogenous parathyroid hormone which has been revealed to promote osteogenesis of mesenchymal stem cells (hMSCs) to alleviate osteoporosis. Currently, the underlying cellular and molecular mechanisms of TPD in treating OP were not fully understood. This study aimed to investigate the roles of non-coding RNA-regulated osteogenic differentiation of hMSCs under TPD treatments. Circular RNA FNDC3B was significantly downregulated, and miRNA-125a-5p was upregulated in primary hMSCs of osteoporosis patients. Moreover, during osteogenesis, expression of circFNDC3B and glutamine metabolism were gradually elevated and miR-125a-5p was suppressed. Silencing circFNDC3B or overexpression of miR-125a-5p remarkedly suppressed the TPD-induced osteogenic differentiation-related genes (ALP, RUNX2, osteocalcin, osteonectin) activity or expression and calcium deposition of hMSCs. Results from RNA pull-down, RNA IP and luciferase assays demonstrated that circFNDC3B sponged miR-125a-5p, which further targeted 3'UTR of glutaminase (GLS), a key enzyme in glutamine metabolism to form a ceRNA regulator network. Rescue experiments demonstrated under TPD treatment, silencing of circFNDC3B significantly upregulated miR-125a-5p expression, blocked GLS expression and inhibited osteogenic differentiation evidenced by the suppressed ALP activity and expressions of osteocalcin, osteonectin and RUNX2. These regulatory phenotypes were further overridden by miR-125a-5p inhibition. In summary, our study demonstrated that TPD treatment promoted osteogenic differentiation of hMSCs by regulating the circFNDC3B-miR-125a-5p-GLS pathway.

Keywords Osteoporosis, Teriparatide, Circular RNA, Glutamine metabolism, Osteogenic differentiation

*Correspondence:
Jiaxin Fu
fujiaxinspine@126.com
[1]Department of Orthopedics, The Third Central Hospital of Tianjin, Tianjin 300170, China
[2]Tianjin Key Laboratory of Extracorporeal Life Support for Critical Diseases, Tianjin 300170, China
[3]Artificial Cell Engineering Technology Research Center, Tianjin 300170, China
[4]Tianjin Institute of Hepatobiliary Disease, Tianjin 300170, China
[5]Department of Orthopedics, The Third Central Hospital of Tianjin, 83 Jintang Road, Hedong District, Tianjin 300170, China

Introduction

Osteoporosis is an identifiable and treatable ailment, characterized by a decrease in bone density and mass, destruction of bone microstructure, and an increased vulnerability to fractures, making the body more prone to fractures [1–3]. There are two main types of osteoporosis: primary and secondary [3, 4]. Primary osteoporosis can be further divided into three types: postmenopausal osteoporosis (type I), senile osteoporosis (type II), and idiopathic osteoporosis (including juvenile type) [5]. Postmenopausal osteoporosis typically manifests within 5–10 years after menopause in women, while senile osteoporosis refers to bone loss in individuals aged over 70 years [6]. Presently, the precise cellular and molecular mechanisms of idiopathic osteoporosis, which predominantly affect teenagers, remain unclear [7].

The essential roles of human multi-potential mesenchymal stem cells (hMSCs) in maintaining and repairing different tissues, including bone, have been widely recognized [8]. Various studies have shown that osteoporosis is caused by a disruption in the balance of osteoblast-promoted osteogenesis and osteoclast-induced bone resorption [9, 10]. Teriparatide (TPD), an FDA-approved therapeutic agent for osteoporosis patients, is a recombinant N-terminal polypeptide (1–34 amino acid) of human PTH [11]. In clinical settings, TPD promotes bone formation by stimulating osteoblast-derived bone formation and inhibiting osteoclast-induced bone resorption, leading to an overall increase in bone mass [12, 13]. However, the precise mechanisms underlying the oncogenic differentiation of hMSCs facilitated by TPD have not been fully elucidated.

Non-coding RNAs, which are RNAs that do not have the ability to code for proteins, are known to play important roles in regulating gene expression and cellular processes [14]. Recent studies have shown that circRNAs interact with other non-coding RNAs, mRNAs, and proteins to regulate the expression of downstream genes [15, 16]. Circular RNAs have been found to have an impact on the progression of osteoporosis [17]. For example, circRNA_0007059 has been identified as a critical regulator of postmenopausal osteoporosis through its interaction with the miR-378/BMP-2 axis [18]. The role and mechanisms of circFNDC3B, a fibronectin type III domain containing 3B circular RNA, in osteoporosis are still unclear [19].

The process of osteogenic differentiation in hMSCs is initiated by hormonal, environmental, and nutritional factors and is important for bone remodeling [20]. It has been discovered in recent studies that metabolic programming plays a crucial role in providing energy and biomaterials during bone remodeling [21], indicating that maintaining cellular metabolism homeostasis is beneficial for osteogenic differentiation of hMSCs. A recent study reported that glutamine catabolism was increased in glutamine catabolism during bone formation [22]. Moreover, inhibition of glutamine metabolism effectively impaired osteogenic differentiation of hMSCs [23], suggesting that glutamine metabolism is essential for osteogenic differentiation.

The objective of this study was to examine the cellular and molecular mechanisms underlying TPD-promoted osteogenesis. Bioinformatics analysis indicated circFNDC3B could associate with miR-125a-5p, which contains binding sequence of GLS 3'UTR region, inspiring us to investigate whether the circFNDC3B-miR-125a-5p-GLS axis exists and functions in osteogenic differentiation. This study will unveil the cellular and molecular mechanisms for the clinical application of TPD in preventing and treating osteoporosis.

Materials and methods

OP patient sample collection and isolation of hMSCs

The Ethics Committee of the Department of Orthopedics at The Third Central Hospital of Tianjin gave approval for this study. Patients with cancers, rheumatoid arthritis, and other metabolic diseases were not included in this study. Osteoporosis was diagnosed by dual-energy X-ray absorptiometry. Both osteoporosis patients ($n=40$) and health controls ($n=40$) provided bone marrow samples, which were promptly frozen in liquid nitrogen and stored at -80 °C. hMSCs were isolated from the bone marrow using techniques outlined in a previous study [24]. Prior to bone marrow collection, informed consent was acquired from all participants.

Cell culture and osteogenic differentiation of hMSCs

The α-Modified Eagle Medium (α-MEM) (HyClone, USA) supplemented with 10% fetal bovine serum (Gibco, USA), 1 x penicillin, 1 x streptomycin, and 0.5 μg/mL of fungizone was used to culture hMSCs in 10-mm plates. The cells were maintained in an incubator at 37 °C with 5% CO_2. Osteogenic differentiation was induced by allowing the cells to grow until they reached 70–80% confluence, after which an osteogenic inducer consisting of 50 μg/mL ascorbic acid (Sigma-Aldrich, USA), 10 mM glycerophosphate (Sigma-Aldrich, USA), and 0.1 μg/mL dexamethasone (Sigma-Aldrich, USA) was applied. The medium was replaced twice a week. To treat the hMSCs, Teriparatide from Sigma-Aldrich (USA) was used at concentrations of 0, 10, and 20 nM for a duration of 24 h.

Cell transfection

hMSCs were pre-plated and cultured for 24 h to reach 60% confluency. Cells were transfected with control siRNA or si circFNDC3B; control miRNA or miR-125a-5p; miRNA inhibitor control or miR-125a-5p inhibitor; control plasmid or pcDNA-GLS; constructed

luciferase vectors using Lipofectamine 2000 (Invitrogen, USA) according to the instructions from the kit. Forty-eight hours after transfection, cells were harvested and used for downstream RT-qPCR or osteogenic differentiation analysis.

Measurements of glutamine metabolism

After transfection or treatment, the glutamine metabolism rate of hMSCs was determined by glutamine uptake and glutaminase activity assays using the Glutamine Assay kit (#MAK438, Sigma-Aldrich, USA) and the Glutaminase (GLS) Activity Assay Kit (ab284547, Abcam, USA) according to the manufacturer's protocols. Assays were conducted in triplicate.

RNA extraction and RT-qPCR

Total RNA was extracted from hMSCs using TRIzol reagent (Invitrogen, Carlsbad, CA, USA) according to strict guidelines. The concentration and purity of the RNA were evaluated through spectrophotometry. The extracted RNA was then converted into cDNA using the Primescript RT kit (TaKaRa, Japan). RT-qPCR was conducted on an ABI Prism 7500 HT Sequence Detection System (Applied Biosystems, USA) using the SYBR premix Ex TaqII kit (TaKaRa, Japan). The RT-qPCR conditions involved heating at 95 °C for 10 min, followed by 40 cycles at 95 °C for 30 s, annealing at 60 °C for 20 s, and extension at 50 °C. For mRNA and circular RNA detection, β-actin was employed as an internal reference. U6 was used as an internal reference for miRNA detection. The relative gene expression was determined using the 2-ΔΔCt method.

Alkaline phosphatase (ALP) activity assay

ALP activity was detected using the Alkaline Phosphatase Assay Kit (#MAK447) from Sigma-Aldrich (Shanghai, China). Post transfection or osteogenic differentiation, hMSCs were collected and lysed by 0.2% Triton X-100. After washing with PBS (phosphate-buffered saline), the cells were incubated with buffers from the kit. Optical density (OD) was read at 405 nm. The relative ALP activity was calculated by the ratio of OD value from experimental group to that from control group.

Alizarin red S staining for calcium deposition

The calcium deposition of hMSCs during osteogenic differentiation was assessed by Alizarin Red S staining assay. hMSCs (1×10^4 cells/well) were seeded in 24-well plates. After transfection and osteogenic induction, cells were washed by PBS, followed by fixation with 4% paraformaldehyde for 15 min. After being exposed to Alizarin Red S solution (1%, pH 4.2) for 10 min at 37 degrees Celsius, the cells were rinsed three times with distilled water before being photographed using a phase-contrast microscope from Leica, Germany.

RNA pull-down assay

Scramble, sense or antisense circFNSC3B oligomers were synthesized and labeled with biotin from RiboBio Co. Ltd (Guangzhou, China). hMSC cell lysates were incubated with individual probe for 2 h at 4 °C. Lysates were incubated with Streptavidin-coupled agarose beads (ThermoFisher, USA) for 1 more hour. After washing the beads with PBS, the amounts of miR-125a-5p from the probe-precipitated RNA complexes were determined by RT-qPCR.

RNA Immunoprecipitation (RNA-IP)

RIP assay was performed using Magna RIPTM RNA-binding protein immunoprecipitation kit (Millipore, USA) following instructions from the kit. Cell lysates from hMSCs were incubated with anti-Ago2 antibody (Sigma-Aldrich, USA) for 4 h at 4 °C. Protein A magnetic beads (Sigma-Aldrich, USA) were added into lysates and incubated for 2 h at 4 °C. The precipitated RNAs were washed out from beads. The amounts of circFNDC3B from the Ago2-precipitated RNAs were determined by RT-qPCR.

Luciferase activity assay

The wild-type circFNDC3B and GLS 3'UTR and the miR-125a-5p binding site mutant circFNDC3B and GLS 3'UTR were cloned into pmiR-GLO vector (Promega, USA). hMSC cells were co-transfected with miR-125a-5p precursor (20 nM) or negative control (20 nM) plus WT- or Mut- circFNDC3B (1 μg) or GLS 3'UTR (1 μg) for 48 h. Cells were lysed and subjected to detection of luciferase activity using a Dual-Luciferase reporter assay kit (Promega, USA).

Western blot

Proteins from hMSCs were extracted using RIPA buffer (Sigma-Aldrich, USA), which was supplied with 1 x protease inhibitor cocktail (ThermoFisher, USA). The lysates were then incubated on ice for 20 min and centrifuged at 10,000 x g for 10 min at 4 oC. The concentration of proteins was determined using the Bradford reagent (Bio-Rad, USA). After denaturation, the protein samples were separated through sodium dodecyl sulphate-polyacrylamide gel electrophoresis (SDS-PAGE) and transferred to PVDF membranes (Millipore, USA). Next, the membranes were blocked with 5% skimmed milk at room temperature for 1 h. They were then washed with PBS and incubated overnight at 4 oC with primary antibodies (anti-GLS, 1:1000, #4970, Cell Signaling, USA; anti-β-actin, 1:1000, #56750, Cell Signaling, USA). After washing, the membranes were incubated with a

secondary horseradish peroxidase (HRP)-labeled antibody (1:3000) for 1 h at room temperature. The protein bands were detected and visualized using a chemiluminescence kit (Sigma-Aldrich, USA).

Statistical analysis

The GraphPad Prism 8.0 (GraphPad Software, USA) was used for all statistical analysis. Data were represented as mean ± SD (Standard Deviation). Student t-test was applied to compare the differences between two groups. One-way analysis of variance (ANOVA) was performed to compare the differences among three or more groups, followed by Post-Hoc Test (Least Significant Difference). Experiments were repeated three times.

Results

circFNDC3B and miR-125a-5p are reversely expressed in osteoporosis patients and hMSCs

We evaluated the expressions of non-coding RNAs in patients with osteoporosis (OP) (Table 1). Using RT-qPCR, we detected low expression of circFNDC3B ($p < 0.001$) in primary hMSCs of OP patients ($n = 40$) compared to healthy controls (Fig. 1A). On the other hand, our miRNA expression screen (data not shown) revealed upregulation of miR-125a-5p, which has been reported to be negatively associated with osteogenesis [25], in hMSCs of OP patients. To investigate the roles of circFNDC3B and miR-125a-5p during hMSC differentiation, we conducted an in vitro osteogenesis model by culturing hMSCs isolated from bone marrow of healthy controls and OP patients for 0, 3, 7, and 10 days. We measured ALP activity (Fig. 1C), expressions of osteocalcin (OCN) (Fig. S1), osteonectin (ON) (Fig. S1B) and the transcription factor RUNX2 (Fig. 1D) as markers of osteogenic differentiation. As expected, we observed opposite expression patterns of circFNDC3B and miR-125a-5p during osteogenesis, with circFNDC3B upregulation (Fig. 1E) and miR-125a-5p downregulation as osteogenic differentiation progressed (Fig. 1F). These findings suggest that circFNDC3B and miR-125a-5p play critical roles in the occurrence and development of OP.

Table 1 Characteristics of OP patients enrolled in this study

Characteristic	Cases	Percentages
Age		
<30	1	2.5%
30-60	12	30%
>60	27	67.5%
Gender		
Male	17	42.5%
Female	23	57.5%
OP Stage		
I	2	5%
II	16	40%
III	17	42.5%
IV	5	12.5%
Smoke		
Never	4	10%
Little	23	57.5%
Heavy	13	32.5%
Mean BMD T score		
Femoral neck	-2.7	
Total hip	-2.9	

circFNDC3B and miR-125a-5p play invert roles in the Teriparatide-promoted osteogenic differentiation of hMSCs

A number of studies have shown that Teriparatide effectively promotes osteogenesis of mesenchymal stem cells, thereby alleviating osteoporosis [11–13]. We then investigated whether the aforementioned non-coding RNAs are involved in the osteogenesis facilitated by TPD. The expression level of circFNDC3B was significantly increased under TPD treatment in hMSCs (Fig. 2A). Conversely, miR-125a-5p was effectively decreased by TPD treatment (Fig. 2B). To confirm the roles of these non-coding RNAs under TPD treatment, circFNDC3B was silenced and miR-125a-5p was overexpressed in hMSCs (Fig. 2C and D). TPD treatment stimulated ALP activity and RUNX2 expression in hMSCs (Fig. 2E and H). Subsequently, silencing of circFNDC3B or overexpression of miR-125a-5p significantly inhibited the TPD-promoted ALP activity (Fig. 2E and F), calcium deposition (Fig. S2A, S2B), and expressions of osteocalcin (Fig. S3A, 3B), osteonectin (Fig. S3C, S3D) and RUNX2 (Fig. 2G and H). In summary, these functional assays demonstrated that circFNDC3B contributes to the osteogenesis of hMSCs, while miR-125a-5p plays the reverse role to circFNDC3B.

Roles of glutamine metabolism of hMSCs in osteogenesis and osteoporosis

To investigate the cellular mechanisms underlying the regulation of non-coding RNA in hMSCs osteogenic differentiation, we assessed the glutamine metabolism of hMSCs during TPD-promoted osteogenesis. The key enzyme in glutamine metabolism, GLS, was significantly downregulated in hMSCs from OP patients (Fig. 3A), suggesting impaired glutamine metabolism in osteoporosis.

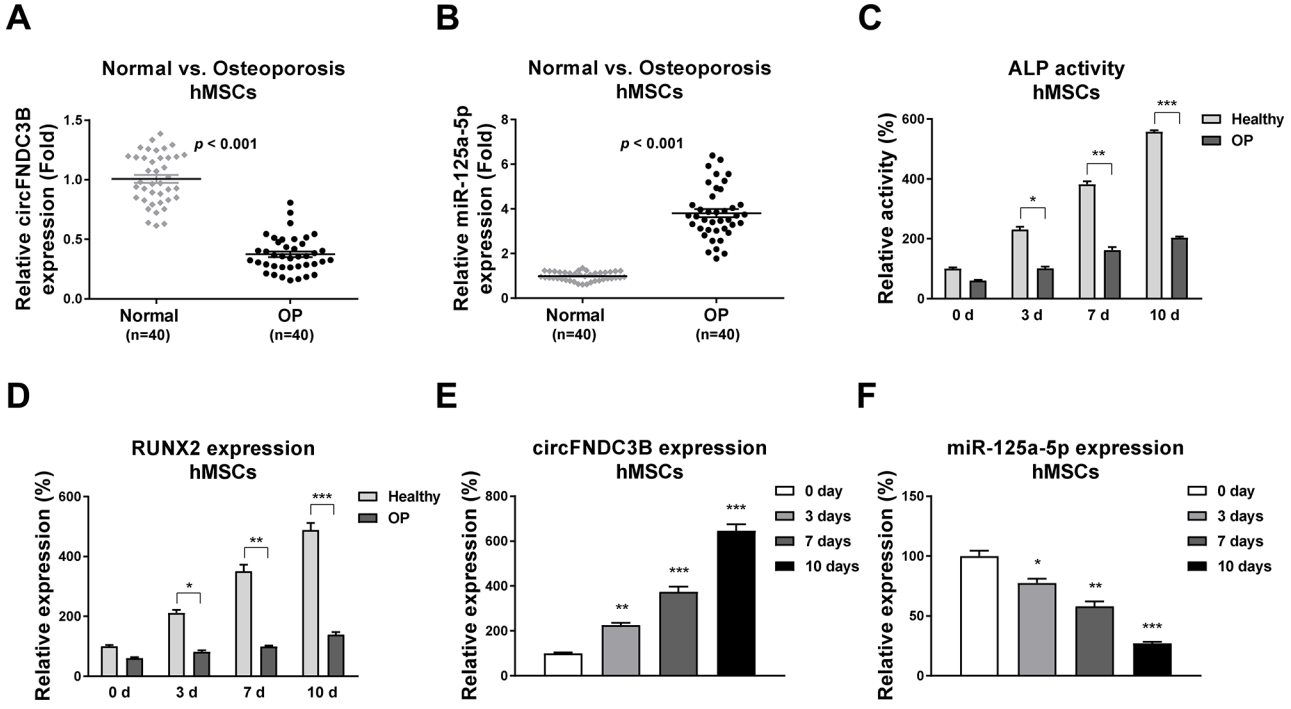

Fig. 1 Expression of circFNDC3B and miR-125a-5p in OP patients and osteogenic differentiation of hMSCs. (**A**) Expression of circFNDC3B and (**B**) miR-125a-5p in hMSCs of patients with osteoporosis and healthy controls detected by RT-qPCR. (**C**) ALP activities and (**D**) RUNX2 expressions were detected in hMSCs from normal and OP patients during osteogenic differentiation. (**E**) Expression of circFNDC3B and (**F**) miR-125a-5p in hMSCs during osteogenic differentiation detected by RT-qPCR. n: number; *, $p < 0.05$; **, $p < 0.01$; ***, $p < 0.001$

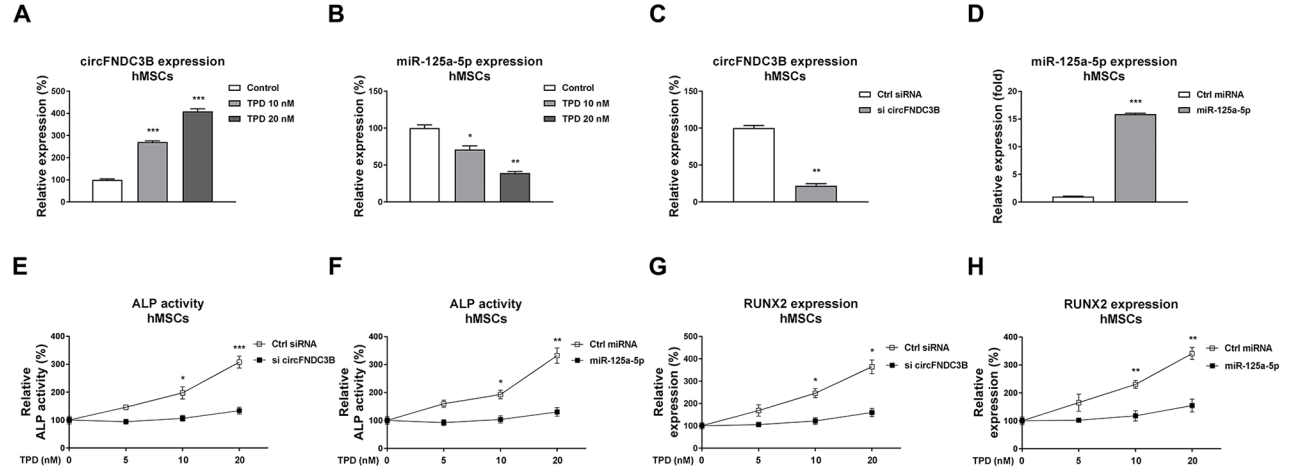

Fig. 2 Roles of circFNDC3B and miR-125a-5p in TPD-promoted osteogenic differentiation of hMSCs. (**A**) Expressions of circFNDC3B and (**B**) miR-125a-5p under TPD treatments. (**C**) hMSCs were transfected with control siRNA or si circFNDC3B, knockdown efficiency of circFNDC3B was examined by RT-qPCR. (**D**) hMSCs were transfected with control miRNA or miR-125a-5p. Expression of miR-125a-5p was detected. (**E**) The circFNDC3B-silenced hMSC cells were treated with TPD at the indicated concentrations, ALP activity was detected. (**F**) The miR-125a-5p-overepressed hMSC cells were treated with TPD at the indicated concentrations, ALP activity was detected. (**G**) RUNX2 expressions were detected by RT-qPCR in circFNDC3B-silenced and (**H**) miR-125a-5p-overepressed hMSCs. *, $p < 0.05$; **, $p < 0.01$; ***, $p < 0.001$

In vitro assays showed that glutamine uptake (Fig. 3B) and glutaminase activity (Fig. 3C) were activated during osteogenesis at 3, 7, and 10 days. Furthermore, GLS expression was significantly upregulated during osteogenesis (Fig. 3D). Inhibiting glutamine metabolism with the GLS inhibitor, BPTES, effectively attenuated ALP activity (Fig. 3E) and expressions of osteocalcin (Fig. S4A), osteonectin (Fig. S4B) and RUNX2 (Fig. 3F), indicating that glutamine metabolism is necessary for hMSCs' osteogenic differentiation. We also investigated the role of glutamine metabolism during TPD-promoted osteogenesis. hMSCs were cultured under low glutamine

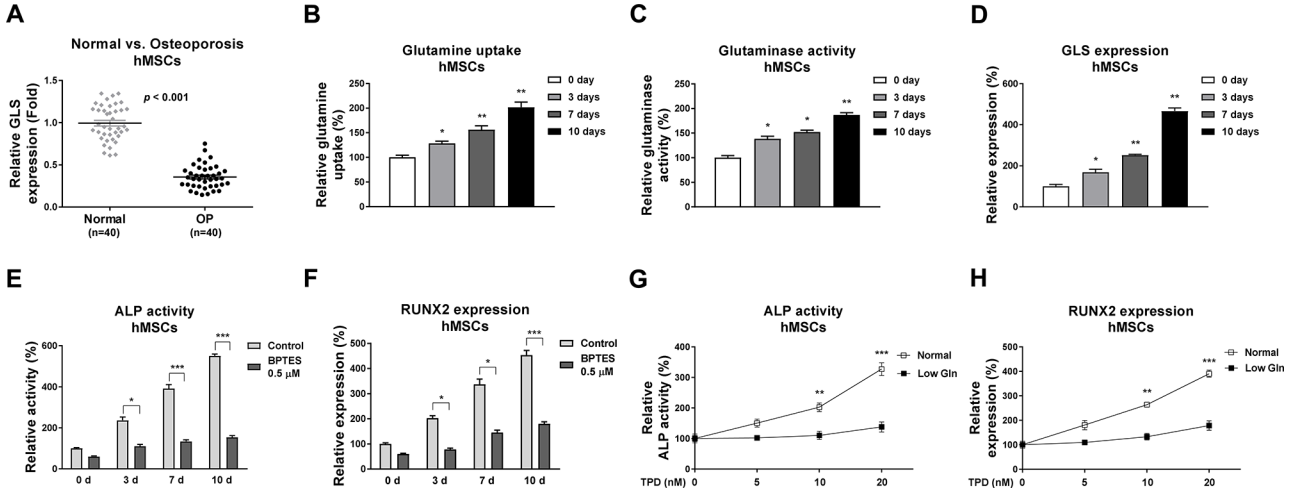

Fig. 3 Roles of glutamine metabolism in TPD-promoted osteogenic differentiation of hMSCs. (**A**) Expression of GLS mRNA in hMSCs of patients with osteoporosis detected by RT-qPCR. (**B**) Glutamine uptake, (**C**) GLS activity and (**D**) GLS mRNA expressions from osteogenic differentiated hMSCs were detected. (**E**) hMSCs were treated with GLS inhibitor, BPTES, ALP activity and (**F**) RUNX2 expression were detected during osteogenic differentiation. (**G**) hMSCs were cultured under low glutamine condition for 2 days. Cells were treated with TPD, ALP activity and (H) RUNX2 expression were detected. n: number; *, $p < 0.05$; **, $p < 0.01$; ***, $p < 0.001$

conditions for 2 days and then treated with TPD for 0, 3, 7, and 10 days. As expected, low glutamine metabolism resulted in dysregulated osteogenesis, as evidenced by diminished ALP activity (Fig. 3G) and downregulated osteocalcin (Fig. S4C), osteonectin (Fig. S4D) and RUNX2 expressions (Fig. 3H). In summary, maintaining glutamine metabolism is beneficial for the osteogenic differentiation of hMSCs.

Glutamine metabolism of hMSCs is reversely regulated by circFNDC3B and miR-125a-5p

Given the above results, which uncovered the roles of circFNDC3B, miR-125a-5p, and glutamine metabolism in the TPD-facilitated osteogenic differentiation of hMSCs, we examined whether these non-coding RNAs directly regulate glutamine metabolism. It appears that silencing circFNDC3B suppressed glutamine uptake (Fig. 4A) and GLS activity (Fig. 4B) of hMSCs. Similar results were obtained with the overexpression of miR-125a-5p, which significantly blocked glutamine metabolism of hMSCs (Fig. 4C and D).

circFNDC3B downregulates miR-125a-5p expression by sponging it in hMSCs

Since circular RNAs function as sponge of miRNAs to block their expressions [17], we assessed whether circFNDC3B associated with miR-125a-5p in hMSCs. Sequence alignments from starBase indicated that circFNDC3B contains putative binding sites of miR-125a-5p (Fig. 5A), indicating miR-125a-5p might be a downstream target of circFNDC3B. Expressions of circFNDC3B and miR-125a-5p were negatively correlated in hMSCs of OP patients (Fig. 5B). Moreover, silencing of circFNDC3B remarkedly upregulated miR-125a-5p in hMSCs (Fig. 5C). To further evaluate whether circFNDC3B is associated with miR-125a-5p, RNA pull-down and RNA IP assays were conducted. Results illustrated that compared with control probe and sense probe precipitation groups, the amount of miR-125a-5p was only enriched in the antisense circFNDC3B prob-precipitated RNA complex (Fig. 5D). In addition, RIP assay revealed that circFNDC3B directly bound to Ago2-associated RNA-induced silencing complexes which were mediated by miRNAs (Fig. S5). Subsequently, overexpression of miR-125a-5p significantly increased the amount of circFNDC3B pulled down by Ago2 (Fig. 5E). The direct binding of miR-125a-5p on predicted sites of circFNDC3B was further verified by luciferase assay which demonstrated that co-transfection of miR-125a-5p and wild type (WT-) circFNDC3B effectively diminished the luciferase activity of hMSCs compared with those from control group and cells co-transfected with miR-125a-5p plus binding site mutant (Mut-) circFNDC3B group (Fig. 5F). Taken together, these results demonstrated that circFNDC3 blocked miR-125a-5p by sponging it in hMSCs.

miR-125a-5p directly targets GLS 3'UTR to suppress osteogenesis

The mRNA targets of miR-125a-5p were subsequently investigated. It was known that microRNAs functioned by binding to the 3'UTR of target mRNAs, which led to inhibition of mRNA activity [17]. Sequence analysis from the starBase service revealed that the 3'UTR of GLS contained binding sites for miR-125a-5p (Fig. 6A). Additionally, there was a negative correlation between the expression of GLS and miR-125a-5p in OP patients,

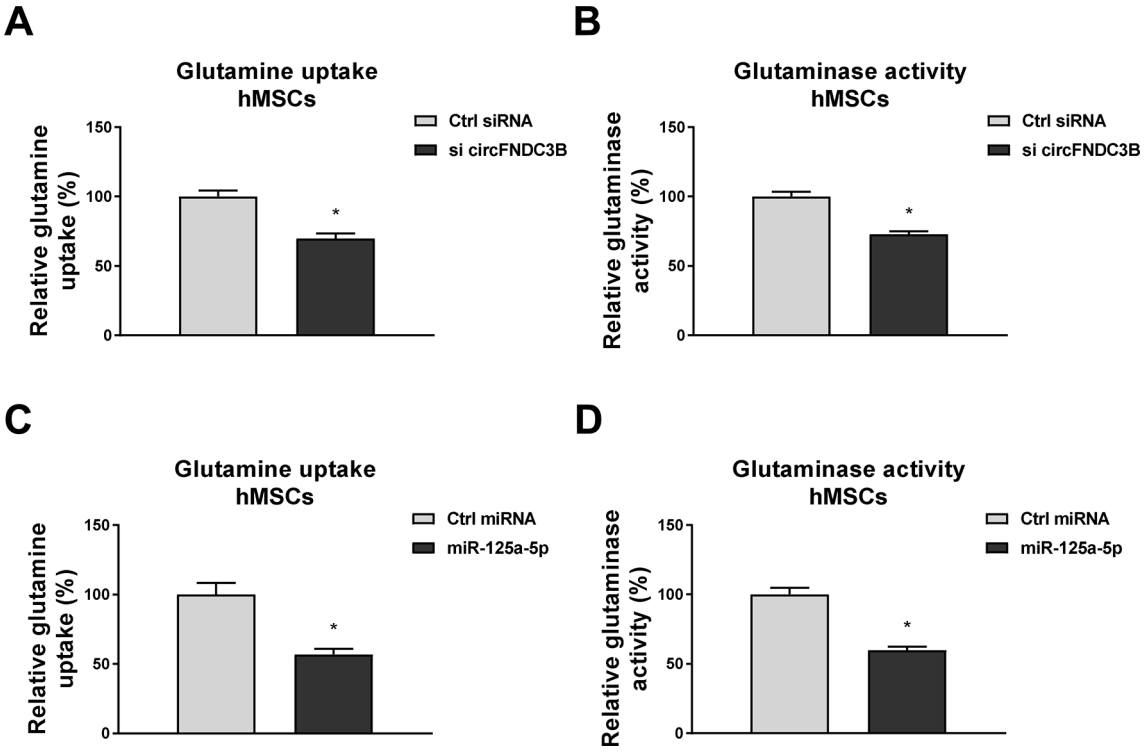

Fig. 4 circFNDC3B and miR-125a-5p reversely regulate glutamine metabolism of hMSCs. (**A**) circFNDC3B was silenced in hMSCs, the glutamine uptake and (**B**) GLS activity were examined. (**C**) miR-125a-5p was overexpressed in hMSCs, the glutamine uptake and (**D**) GLS activity were examined. *, $p < 0.05$

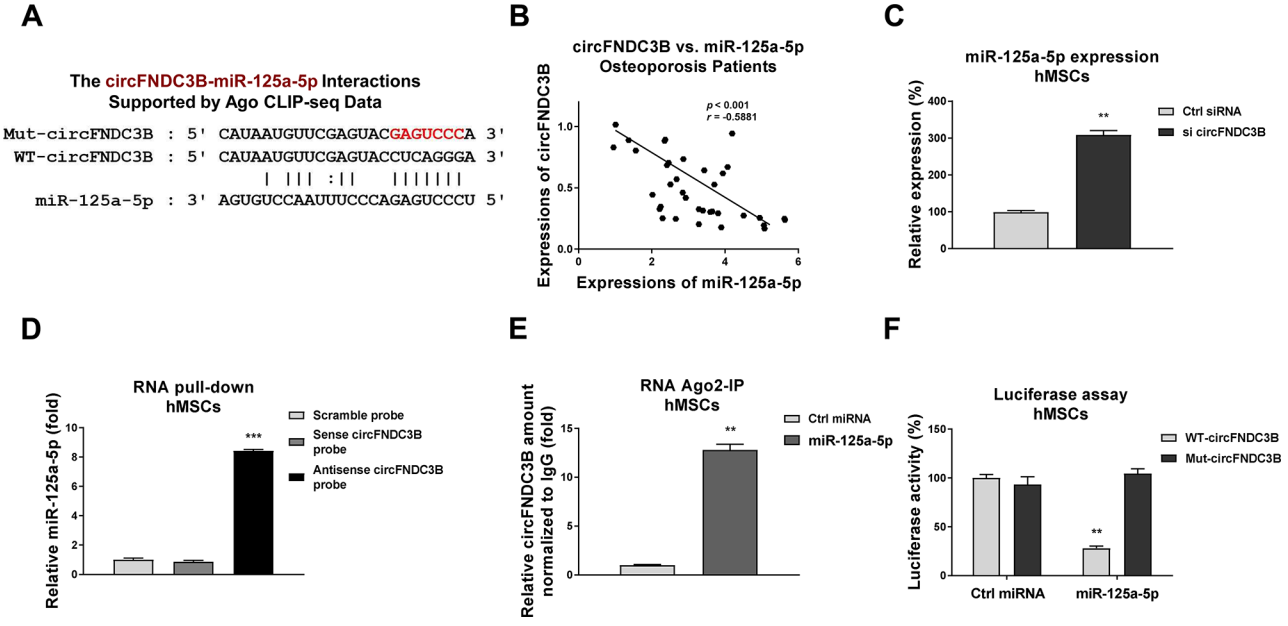

Fig. 5 circFNDC3B sponges miR-125a-5p to downregulate it in hMSCs. (**A**) Prediction of the circFNDC3B/miR-125a-5p association from starBase. (**B**) Negative correlation between circFNDC3B and miR-125a-5p was detected in hMSCs of OP patients. (**C**) Expression of miR-125a-5p was detected in circFNDC3B-silenced hMSCs. (**D**) RNA pull-down assay was conducted in hMSCs using the biotin-labeled scramble, sense or antisense circFNDC3B probe to pull down miR-125a-5p in cell lysates. Amount of miR-125a-5p in RNA complex was determined by RT-qPCR. (**E**) Anti-Ago2 RIP was performed in hMSCs cells which were transfected with control miRNA or miR-125a-5p. Amount of circFNDC3B in the Ago2-precipitated complex was detected by RT-qPCR. (F) Luciferase assay was conducted in hMSCs through co-transfection of control miRNA or miR-125a-5p with WT- or Mut- circFNDC3B. **, $p < 0.01$; ***, $p < 0.001$

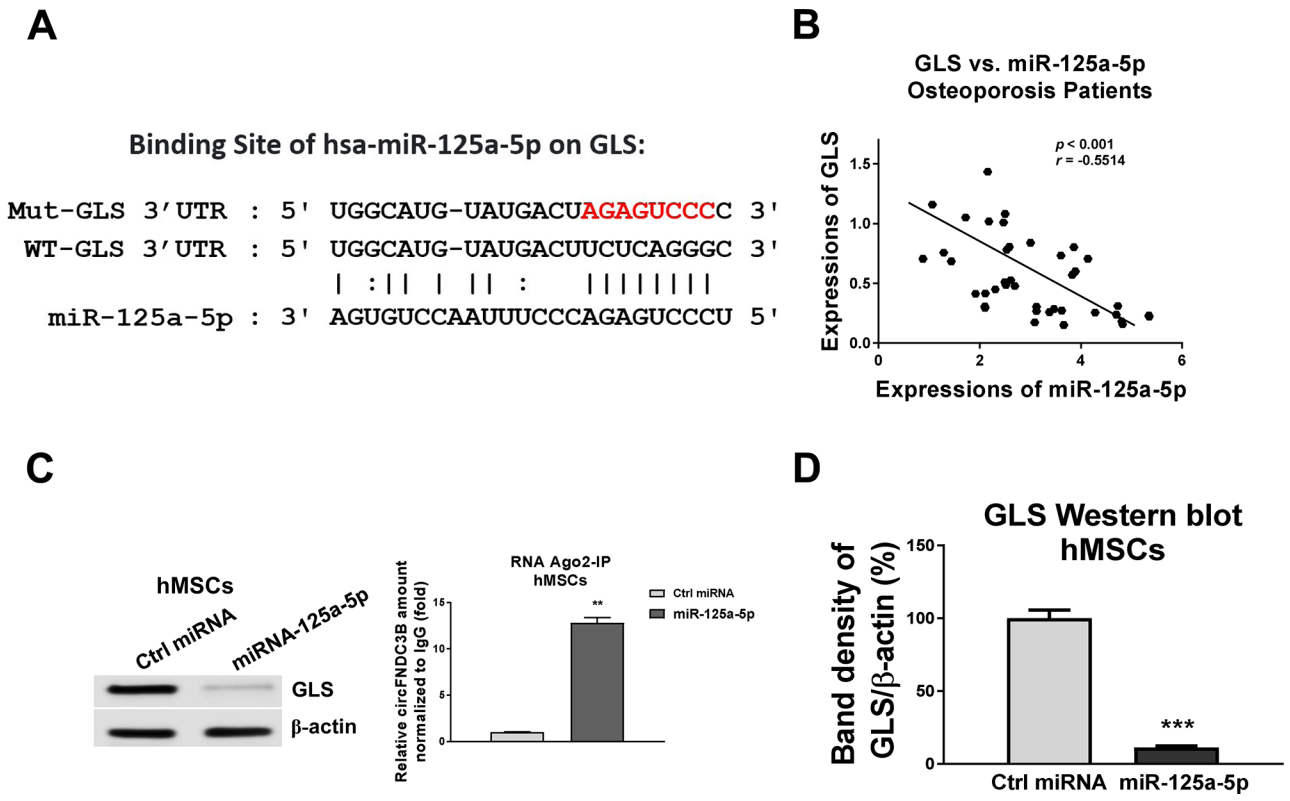

Fig. 6 miR-125a-5p directly targets 3'UTR of GLS in hMSCs. (**A**) Prediction of the miR-125a-5p/GLS 3'UTR association from starBase. (**B**) Negative correlation between GLS mRNA and miR-125a-5p was detected in hMSCs of OP patients. (**C**) hMSCs were transfected with control miRNA or miR-125a-5p, protein expression of GLS was detected by Western blot. (**D**) Luciferase assay was conducted in hMSCs through co-transfection of control miRNA or miR-125a-5p with WT- or Mut- GLS 3'UTR. **, $p < 0.01$; ***, $p < 0.001$

as analyzed by Pearson's correlation coefficient (Fig. 6B). These findings suggest that miR-125a-5p may directly target GLS in hMSCs. To test this hypothesis, we transfected hMSC cells with either control miRNAs or miR-125a-5p. As expected, overexpression of miR-125a-5p significantly reduced the expression of GLS protein (Fig. 6C). A luciferase reporter assay was then conducted to determine whether miR-125a-5p directly binds to the predicted 3'UTR regions of GLS. Results from Fig. 6D showed that transfection of miR-125a-5p significantly decreased the luciferase activity of cells that were co-transfected with a vector containing the wild-type GLS 3'UTR. On the other hand, co-transfection with control miRNAs or miR-125a-5p plus a mutant GLS 3'UTR that lacked the binding site had no significant effect on luciferase activity in hMSC cells (Fig. 6D).

Rescue experiments were conducted to validate whether miR-125a-5p-mediated osteogenic differentiation occurred through the targeting of GLS. Human mesenchymal stem cells (hMSCs) were co-transfected with control miRNA, miR-125a-5p alone, or miR-125a-5p in combination with GLS (Fig. 7A). The transfection of GLS into miR-125a-5p-overexpressing hMSCs effectively restored the expression of GLS (Fig. 7A). Consequently, hMSC cells with the rescue of GLS displayed restored glutamine metabolism (Fig. 7B), ALP activity (Fig. 7C), calcium deposition (Fig. S6) and expressions of osteocalcin (Fig. S7A), osteonectin (Fig. S7B) and RUNX2 (Fig. 7D) during osteogenic differentiation. The rescue experiments confirmed that miR-125a-5p hindered osteogenic differentiation by targeting GLS.

Teriparatide facilitates osteogenesis of hMSCs through modulating the circFNDC3B-miR-125a-5p-GLS pathway

Based on the results above, we evaluated whether TPD promoted osteogenic differentiation of hMSCs through non-coding RNA-mediated glutamine metabolism. hMSCs were transfected with control, circFNDC3B siRNA alone, or circFNDC3B siRNA plus miR-125a-5p antisense. Inhibition of miR-125a-5p successfully reversed the circFNDC3B silencing-induced miR-125a-5p (Fig. 8A) and GLS (Fig. 8B) expressions as confirmed by RT-qPCR and Western blot analysis, respectively. Consistent results were obtained showing that the circFNDC3B siRNA plus miR-125a-5p inhibitor transfected cells had restored glutamine uptake (Fig. 8C) and GLS activity (Fig. 8D) similar to those of the control cells. Importantly, under TPD treatment, silencing of

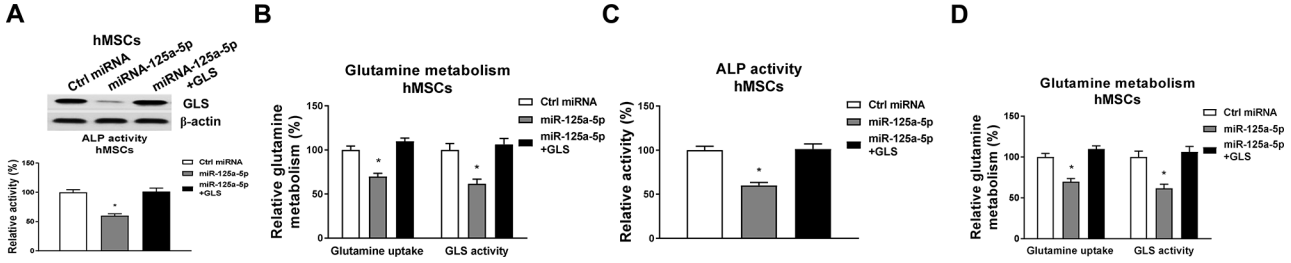

Fig. 7 Recovery of GLS rescues the miR-125a-5p-inhibited glutamine metabolism and osteogenic differentiation of hMSCs. (**A**) hMSCs were transfected with control miRNA, miR-125a-5p alone or miR-125a-5p plus GLS overexpression vector, protein expression of GLS was detected by Western blot. (**B**) Glutamine metabolism, (**C**) ALP activity and (**D**) RUNX2 expression during osteogenic differentiation were detected in the above cells. *, $p < 0.05$; **, $p < 0.01$

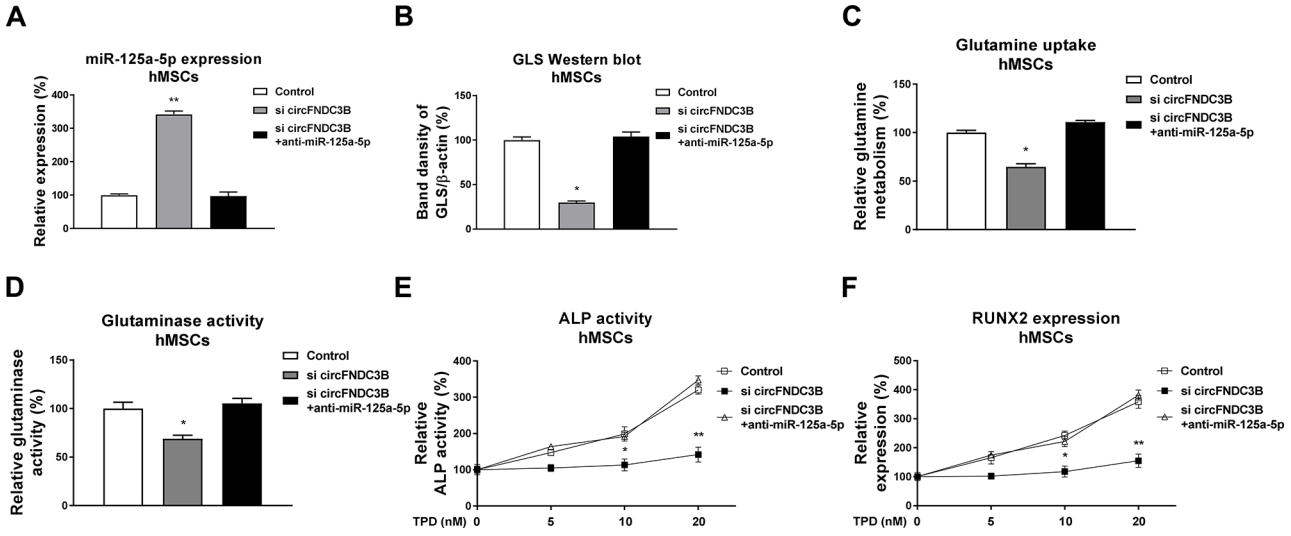

Fig. 8 Roles of the circFNDC3B-miR-125a-5p-GLS axis in the TPD-promoted osteogenic differentiation of hMSCs. (**A**) hMSCs were transfected with control siRNA, si circFNDC3B alone or si circFNDC3B plus miR-125a-5p inhibitor. miR-125a-5p and (**B**) protein expression of GLS were detected by RT-qPCR and Western blot, respectively. (**C**) Glutamine uptake and (**D**) GLS activity from the above transfected cells were detected. (**E**) The above transfected cells were treated with TPD, ALP activity and (**D**) RUNX2 expression were detected in the above cells. *, $p < 0.05$; **, $p < 0.01$; ***, $p < 0.001$

circFNDC3B significantly hindered ALP activity (Fig. 8E) and expressions of osteocalcin (Fig. S8A), osteonectin (Fig. S8B) and RUNX2 (Fig. 8F). These regulatory phenotypes were further reversed by miR-125a-5p inhibition (Fig. 8E and F). In summary, these results confirm that the circFNDC3B-miR-125a-5p-GLS pathway plays a crucial role downstream of TPD treatment.

Discussion

Osteoporosis is characterized by a decrease in bone density and bone mass, the destruction of bone microstructure, and an increase in bone fragility [1, 2]. Primary osteoporosis can be divided into three types: postmenopausal osteoporosis (type I), senile osteoporosis (type II), and idiopathic osteoporosis (including juvenile type) [3–5]. Currently, the cellular and molecular mechanisms of idiopathic osteoporosis, which primarily affect adolescents, are still unknown. The bone remodeling unit consists of different types of cells, either osteoblasts or osteoclasts lineage [8]. The mesenchymal progenitors, which produce osteoblasts and eventually become bone lining cells or osteocytes, are part of the osteoblast lineage, while the osteoclast lineage includes mature osteoclasts and their macrophage precursors [8, 9]. Therefore, it is crucial to discover the genes that regulate the activities of both osteoblasts and osteoclasts.

The proper regulation and coordination of differentiation and function of both cell lineages are crucial for maintaining the adult skeleton, as it couples bone resorption to bone formation [8]. The main cause of OP is the imbalance in the generation of osteoblast and osteoclast cells [10]. This study aimed to investigate the cellular and molecular mechanisms of osteogenic differentiation from hMSCs with TPD treatment. Results revealed a significant attenuation of glutamine metabolism and circFNDC3B in hMSCs from OP patients. Conversely, miR-125a-5p was significantly upregulated in OP patients. During in vitro osteogenesis, expression of circFNDC3B was significantly induced and miR-125a-5p was remarkedly downregulated, indicating that circFNDC3B and

miR-125a-5p have opposite roles and could serve as diagnostic biomarkers for osteogenesis.

Teriparatide is a polypeptide drug derived from parathyroid hormone [12], and it has recently been approved by the FDA for treating OP [12]. The drug stimulates the formation of bones by encouraging the creation of osteoblasts and preventing osteoblasts from dying [13]. However, the exact mechanisms of how Teriparatide regulates osteogenesis are not completely understood. Our study demonstrated that Teriparatide treatments increase the activity of cellular ALP and the expression of RUNX2, osteocalcin and osteonectin in hMSCs. Additionally, the expression of circFNDC3B significantly increased, while the expression of miR-125a-5p was blocked under Teriparatide treatment. Consequently, when we silenced miR-FNDC3B or overexpressed miR-125a-5p, we effectively counteracted the osteogenic differentiation promoted by Teriparatide in hMSCs. These results suggest that circFNDC3B and miR-125a-5p are downstream effectors of Teriparatide during osteogenesis.

Studies have accumulated evidence indicating that circular RNAs and miRNAs play crucial roles in the progression of OP [26]. The discovery of OP-regulated noncoding RNAs that have critical functions has also been made [16]. The known function of circRNAs as cytoplasmic sponges for miRNAs, forming competing endogenous RNAs (ceRNA) [17], has been reported to contribute to the progression of OP. An example of this is the alleviation of osteoporosis progression by CircRNA_0001795, which acts as a sponge for miRNA-339-5p [27]. In this study, bioinformatics analysis indicated that circFNDC3B is associated with miR-125a-5p. Subsequent RNA pull-down, RNA immunoprecipitation, and luciferase assays confirmed that circFNDC3B directly sponges miR-125a-5p in hMSCs. Moreover, the glutamine metabolism key enzyme, GLS, was identified as a target of miR-125a-5p in hMSCs through Western blot and luciferase assays. The restoration of GLS expression in miR-125a-5p-overexpressing hMSCs cells successfully reversed the inhibition of ALP activity and RUNX2 expression by miR-125a-5p. Importantly, under TPD treatment, blocking circFNDC3B significantly upregulated miR-125a-5p expression, decreased GLS expression, and inhibited osteogenic differentiation, as evidenced by suppressed ALP activity and downregulation of osteocalcin, osteonectin and RUNX2. These regulatory effects were further reversed by miR-125a-5p inhibition. However, it is worth noting that the molecular mechanisms discovered in this study need to be further validated using an in vivo osteogenesis model.

In summary, this study showed that the circFNDC3B-miR-125a-5p-GLS pathway is regulated by TPD treatment, resulting in the promotion of osteogenic differentiation in hMSCs. Our findings establish a cellular and molecular foundation for the potential use of TPD in preventing and treating osteoporosis.

Supplementary Information

The online version contains supplementary material available at https://doi.org/10.1186/s12891-025-08505-2.

Supplementary Material 1: Expressions of osteocalcin and osteonectin were detected in hMSCs from normal and OP patients during osteogenic differentiation. *, $p < 0.05$; **, $p < 0.01$; ***, $p < 0.001$

Supplementary Material 2: Alizarin Red S staining for detection of calcium deposition in hMSCs. (A) hMSCs were transfected with control siRNA or si circFNDC3B or (B) control miRNA or miR-125a-5p for 48 h, followed by treating with TPD at 20 nM. Calcium deposition was measured by Alizarin Red S staining

Supplementary Material 3: Effects of circFNDC3B knockdown or miR-125a-5p overexpression on expressions of osteocalcin and osteonectin in hMSCs under TPD treatment. (A) hMSCs were transfected with control siRNA or si circFNDC3B, followed by TPD treatments at the indicated concentrations. Expression of osteocalcin was detected. (B) The miR-125a-5p-overepressed hMSC cells were treated with TPD at the indicated concentrations, expression of osteocalcin was detected. (C) Osteonectin expressions were detected in circFNDC3B-silenced and (D) miR-125a-5p-overepressed hMSCs. *, $p < 0.05$; **, $p < 0.01$

Supplementary Material 4: Roles of glutamine metabolism in expressions of osteocalcin and osteonectin in hMSC cells under osteogenic differentiation and TPD treatment. (A) hMSCs were treated with BPTES, followed by osteogenic differentiation induction. Expressions of osteocalcin and (B) osteonectin were examined. (C) hMSCs were cultured under normal or low glutamine condition, followed by treating with TPD at the indicated concentrations. Expressions of osteocalcin and (D) osteonectin were examined. *, $p < 0.05$; **, $p < 0.01$; ***, $p < 0.001$

Supplementary Material 5: RIP was performed using Anti-Ago2 antibody in hMSC cell lysates. Amount of circFNDC3B was detected by RT-qPCR.

Supplementary Material 6: Alizarin Red S staining for detection of calcium deposition in hMSCs. (A) hMSCs were transfected with control miRNA, miR-125a-5p alone or miR-125a-5p plus GLS for 48 h. Cells were cultured under osteogenesis condition. Calcium deposition was measured by Alizarin Red S staining

Supplementary Material 7: Effects of GLS restoration in miR-125a-5p-overexpressed hMSCs on expressions of osteocalcin and osteonectin. (A) hMSCs were transfected with control miRNA, miR-125a-5p alone or miR-125a-5p plus GLS overexpression vector, expressions osteocalcin and (B) osteonectin were detected. *, $p < 0.05$

Supplementary Material 8: Expressions of osteocalcin and osteonectin were regulating by the circFNDC3B-miR-125a-5p-GLS axis in TPD-promoted osteogenic differentiation of hMSCs. (A) hMSCs were transfected with control siRNA, si circFNDC3B alone or si circFNDC3B plus miR-125a-5p inhibitor, expressions of osteocalcin and (B) osteonectin were detected. *, $p < 0.05$; **, $p < 0.01$

Supplementary Material 9

Acknowledgements

None.

Author contributions

J.X.F. and Zh. L. designed the experiments. J.X.F. Zh. L. G.X.Zh. and Ch.Zh. carried out experiments and analyzed data. J.X.F. reviewed the data and wrote the manuscript. All authors participated into the manuscript preparation.

Funding

This study was supported by an internal basic medical research funding resource from department of orthopedics, the Third Central Hospital of Tianjin, Tianjin, China.

Data availability
The datasets used and/or analyzed during the current study are available from the corresponding author upon reasonable request.

Declarations

Human ethics and consent to participate declarations
This study was approved by the Ethics Committee of the Department of Orthopedics at The Third Central Hospital of Tianjin and conducted in compliance with the Helsinki Declaration. Prior to bone marrow collection, informed consent was acquired from all participants.

Consent for publication
Not Applicable.

Competing interests
The authors declare no competing interests.

Received: 29 December 2023 / Accepted: 6 March 2025
Published online: 17 March 2025

References

1. Gopinath V, Osteoporosis. Med Clin North Am. 2023;107(2):213–25.
2. Foessl I, Dimai HP, Obermayer-Pietsch B. Long-term and sequential treatment for osteoporosis. Nat Rev Endocrinol. 2023;19(9):520–33.
3. Harris K, Zagar CA, Lawrence KV. Osteoporosis: common questions and answers. Am Fam Physician. 2023;107(3):238–46.
4. LeBoff MS, Greenspan SL, Insogna KL, Lewiecki EM, Saag KG, Singer AJ, Siris ES. The clinician's guide to prevention and treatment of osteoporosis. Osteoporos Int. 2022;33(10):2049–102.
5. Gregson CL, Armstrong DJ, Bowden J, Cooper C, Edwards J, Gittoes NJL, Harvey N, Kanis J, Leyland S, Low R, McCloskey E, Moss K, Parker J, Paskins Z, Poole K, Reid DM, Stone M, Thomson J, Vine N, Compston J. UK clinical guideline for the prevention and treatment of osteoporosis. Arch Osteoporos. 2022;17(1):58.
6. Sabri SA, Chavarria JC, Ackert-Bicknell C, Swanson C, Burger E. Osteoporosis: An Update on Screening, Diagnosis, Evaluation, and Treatment. Orthopedics. 2023 Jan-Feb;46(1):e20-e26.
7. Ciancia S, Högler W, Sakkers RJB, Appelman-Dijkstra NM, Boot AM, Sas TCJ, Renes JS. Osteoporosis in children and adolescents: how to treat and monitor? Eur J Pediatr. 2023;182(2):501–11.
8. Mazzoni E, Iaquinta MR, Mosaico M, De Pace R, D'Agostino A, Tognon M, Martini F. Human mesenchymal stem cells and innovative scaffolds for bone tissue engineering applications. Tissue Eng Part B Rev. 2023;29(5):514–31.
9. Mushahary D, Spittler A, Kasper C, Weber V, Charwat V. Isolation, cultivation, and characterization of human mesenchymal stem cells. Cytometry A. 2018;93(1):19–31.
10. Cai H, Zou J, Wang W, Yang A. BMP2 induces hMSC osteogenesis and matrix remodeling. Mol Med Rep. 2021;23(2):125.
11. Ayers C, Kansagara D, Lazur B, Fu R, Kwon A, Harrod C. Effectiveness and safety of treatments to prevent fractures in people with low bone mass or primary osteoporosis: A living systematic review and network Meta-analysis for the American college of physicians. Ann Intern Med. 2023;176(2):182–95.
12. Reid IR, Billington EO. Drug therapy for osteoporosis in older adults. Lancet. 2022;399(10329):1080–92.
13. Blick SK, Dhillon S, Keam SJ. Teriparatide: a review of its use in osteoporosis. Drugs. 2008;68(18):2709–37.
14. Panni S, Lovering RC, Porras P, Orchard S. Non-coding RNA regulatory networks. Biochim Biophys Acta Gene Regul Mech. 2020;1863(6):194417.
15. Zhou WY, Cai ZR, Liu J, Wang DS, Ju HQ, Xu RH. Circular RNA: metabolism, functions and interactions with proteins. Mol Cancer. 2020;19(1):172.
16. Yang Y, Yujiao W, Fang W, Linhui Y, Ziqi G, Zhichen W, Zirui W, Shengwang W. The roles of MiRNA, LncRNA and circrna in the development of osteoporosis. Biol Res. 2020;53(1):40.
17. Gao M, Zhang Z, Sun J, Li B, Li Y. The roles of circRNA-miRNA-mRNA networks in the development and treatment of osteoporosis. Front Endocrinol (Lausanne). 2022;13:945310.
18. Liu S, Wang C, Bai J, Li X, Yuan J, Shi Z, Mao N. Involvement of CircRNA_0007059 in the regulation of postmenopausal osteoporosis by promoting the microRNA-378/BMP-2 axis. Cell Biol Int. 2021;45(2):447–55.
19. Li X, Wang C, Zhang H, Li Y, Hou D, Liu D, Xu R, Cheng J, Liu L, Fu Y, Ye J, Jiang H. circFNDC3B accelerates vasculature formation and metastasis in oral squamous cell carcinoma. Cancer Res. 2023;83(9):1459–75.
20. Wang J, Wang T, Zhang F, Zhang Y, Guo Y, Jiang X, Yang B. Roles of circular RNAs in osteogenic differentiation of bone marrow mesenchymal stem cells (Review). Mol Med Rep. 2022;26(1):227.
21. Smith CO, Eliseev RA. Energy metabolism during osteogenic differentiation: the role of Akt. Stem Cells Dev. 2021;30(3):149–62.
22. Karner CM, Esen E, Okunade AL, Patterson BW, Long F. Increased glutamine catabolism mediates bone anabolism in response to WNT signaling. J Clin Invest. 2015;125(2):551–62.
23. Chen Y, Yang YR, Fan XL, Lin P, Yang H, Chen XZ, Xu XD. miR-206 inhibits osteogenic differentiation of bone marrow mesenchymal stem cells by targeting glutaminase. Biosci Rep. 2019;39(3):BSR20181108.
24. Feng J, Wang JX, Li CH. LncRNA GAS5 overexpression alleviates the development of osteoporosis through promoting osteogenic differentiation of MSCs via targeting microRNA-498 to regulate RUNX2. Eur Rev Med Pharmacol Sci. 2019;23(18):7757–65.
25. Sun L, Lian JX, Meng S. MiR-125a-5p promotes osteoclastogenesis by targeting TNFRSF1B. Cell Mol Biol Lett. 2019;24:23.
26. Moura SR, Fernandes MJ, Santos SG, Almeida MI. Circular RNAs: promising targets in osteoporosis. Curr Osteoporos Rep. 2023;21(3):289–302.
27. Li M, Li C, Zheng H, Zhou Z, Yang W, Gong Y, Wu X, Li L. CircRNA_0001795 sponges miRNA-339-5p to regulate yes-associated protein 1 expression and attenuate osteoporosis progression. Bioengineered. 2022;13(2):2803–15.

Publisher's note